Experimental Assessment of Tandem-Hopped Radar and Communications (THoRaCs)

Brandon Ravenscroft[1], Patrick M. McCormick[2], Shannon Blunt[1], Erik S. Perrins[3], Cenk Sahin[2], Justin G. Metcalf[4]
[1]Radar Systems Lab (RSL), University of Kansas, Lawrence, KS
[2]Communications & Signal Processing Lab (CSPL), University of Kansas, Lawrence, KS
[3]Sensors Directorate, Air Force Research Laboratory (AFRL), Wright-Patterson AFB, OH
[4]Radar Innovations Lab, University of Oklahoma, Norman, OK

***Abstract*—A dual-function radar/communication emission scheme was recently developed in which undistorted information-bearing OFDM subcarriers are embedded into the constant amplitude and spectrally well-contained structure of FM noise radar waveforms via a two-stage optimization process. This power-efficient formulation is amenable to high-power amplification on transmit and subsequent demodulation of the embedded communication symbols through standard OFDM receive processing. Here the individual attributes of the emission are experimentally evaluated through free-space transmission followed by capture of the reflected radar echoes along with separate capture and demodulation by a communication receiver.**

Keywords—dual-function radar/communications, spectrum sharing, FM noise radar, waveform diversity

I. INTRODUCTION

Myriad different techniques for radar and communication spectrum sharing have emerged in recent years (e.g. [1-3] and references therein) due to growing congestion, increased competition for RF spectrum [4], and to explore the prospective benefits of dual/multi-function operation. One such multi-function approach was developed in [5, 6] whereby a frequency-hopping spread-spectrum (FH-SS) strategy is leveraged to construct notches in the transmitted spectrum of a radar, with information-bearing subcarriers based on orthogonal frequency division multiplexing (OFDM) then placed within these notches. Denoted as tandem-hopped radar and communications (THoRaCs), since the spectral notches and subcarriers move about the radar spectrum in tandem, the approach was subsequently modified in [7] to form a single power-efficient waveform.

The power efficient formulation was achieved by imposing the constant amplitude structure of FM upon the entire composite radar/communication signal, while still maintaining a faithful representation of the OFDM subcarriers (or at least as close to as possible). Since the inclusion of an information-bearing signal necessitates that the waveform be free to vary, this arrangement can only be accomplished by allowing the composite signal to become a form of FM noise, other variations of which [8-14] have been experimentally demonstrated to provide much greater design freedom for radar as well.

While the approaches in [6] and [7] were referred to as THoRaCs and (power efficient) PE-THoRaCs, respectively, for the sake of convenience we shall use the former (and simpler) name for the latter from this point forward as well. Thus the focus of this paper is on the experimental evaluation of the THoRaCs emission scheme from the radar and communication perspectives. It is shown that the physical THoRaCs waveform is consistent with other FM noise radar emissions in that it can achieve low autocorrelation sidelobes (particularly after coherent integration via subsequent Doppler processing), it has constant amplitude (the reason for good power efficiency), and it possesses good spectral containment (a by-product of the FM signal structure). The communication attribute of this waveform is more complicated, however, due to the potential for symbol distortion during the waveform design process.

II. THORACS WAVEFORM OPTIMIZATION

First, a quick clarification is in order to avoid possible confusion. The incorporation of an OFDM signal into an FM "wrapper" signal might initially lead one to think that it is a form of constant-envelope OFDM (CE-OFDM) [15-17] in which the OFDM component is placed in the exponent of the FM structure in some manner akin to

$$s(t) = \exp\left(j\, h\{r(t)\} \right) = \exp\left(j\phi(t) \right). \tag{1}$$

Here $r(t)$ is the standard OFDM combination of symbol-weighted subcarriers (defined explicitly below) and $h\{\bullet\}$ is some operation such as integration [14], thereby resulting in the continuous, differentiable, instantaneous phase function $\phi(t)$. However, this type of formulation tends to require complicated symbol decoding upon receive.

In contrast to signaling schemes like (1), the THoRaCs formulation produces information-bearing radar waveforms that adhere to the arrangement

$$s(t) = r(t) + e(t) = \exp\left(j\phi(t) \right), \tag{2}$$

where the $e(t)$ term corresponds to the "excess signal" that is required for the OFDM signal $r(t)$ to be subsumed into the FM structure of $s(t)$ in this additive manner. The THoRaCs construction from [7], which is briefly reviewed below, has a final stage that forces adherence to the right-hand side of (2), and may therefore induce some distortion of the intended OFDM signal $r(t)$ if the excess signal $e(t)$ does not possess sufficient degrees of freedom with which to compensate.

To design a coherent processing interval (CPI) of signals according to (2), consider M pulsed FM waveforms having 3-dB bandwidth B and pulse width T. Within each pulse we wish to embed N OFDM subcarriers that are independently modulated with communication symbols drawn from an arbitrary quadrature amplitude modulation (QAM) constellation. Each of these unique waveforms is designed to approximate a desired power spectrum $|G(f)|^2$ whose inverse Fourier transform corresponds to an autocorrelation with relatively low sidelobes. While the choice of power spectrum is also arbitrary, a Gaussian shape is used here because the associated autocorrelation provides low sidelobes in practice [5-8, 10-14].

For the mth pulse, specified over $-T/2 \le t \le +T/2$, the weighted OFDM communication signal is defined as

This work was supported by the Office of Naval Research under Contract #N00014-16-C-2029 and by a subcontract with Matrix Research, Inc. for the Air Force Research Laboratory under Prime Contract #FA8650-14-D-1722. DISTRIBUTION STATEMENT A. Approved for Public Release.
978-1-7281-2660-9/19/$31.00 ©2019 IEEE

$$r_m(t) = \sum_{n=0}^{N-1} a_{m,n} \left| c_{m,n} \right| \exp\left[j\left(2\pi f_{m,n} t + \angle c_{m,n} \right) \right], \quad (3)$$

where $f_{m,n}$ is the frequency of the nth subcarrier, the QAM symbol modulated onto the nth subcarrier is $c_{m,n}$, and $\angle(\bullet)$ extracts the phase of the argument. In addition to the standard OFDM amplitude scaling (for higher-order QAM), the term $a_{m,n}$ is imposed on the nth subcarrier so that, in the expectation over the possible QAM symbols for that subcarrier, the desired waveform power spectrum $|G(f)|^2$ is still maintained.

Given a random FM waveform initialization $s_{0,m}(t)$, the waveform optimization process is then performed by repeatedly applying the sequence of projections [7]

$$b_{k,m}(t) = \mathbb{F}^{-1}\left\{ \left| G(f) \right| \exp\left(j \angle \mathbb{F}\left\{ s_{k,m}(t) \right\} \right) \right\}, \quad (4)$$

$$\tilde{b}_{k,m}(t) = P_{\perp r_m}\left\{ b_{k,m}(t) \right\} + r_m(t), \quad (5)$$

and

$$s_{k+1,m}(t) = \begin{cases} \exp\left(j \angle \tilde{b}_{k,m}(t) \right) & |t| \le T/2 \\ 0 & |t| > T/2 \end{cases}, \quad (6)$$

where $\mathbb{F}$ and $\mathbb{F}^{-1}$ represent the Fourier and inverse Fourier transforms, respectively, and the operator $P_{\perp r_m}\{\bullet\}$ projects the argument onto the orthogonal complement of the subcarrier frequencies comprising r_m. Once this sequence of projections has been applied K times (or based on some stopping criterion), then only the projections (5) and (6) are repeated another L times since any subsequent deviation from the desired spectrum shape in (4) tends to be negligible and we wish to maximize the degree to which the OFDM signal is faithfully represented.

Note that, as shown in [7], if the number of subcarriers N is too large a fraction of the waveform time-bandwidth product BT, the waveform design process above induces distortion of the OFDM component as a result of imposing the structure of (2). Further, because (4)-(6) are performed in a discretized manner in a processor, it is necessary to ensure that sufficient over-sampling relative to 3-dB bandwidth B is provided so that adequate signal fidelity is preserved (i.e. aliasing is minimized, since the finite pulse width cannot be bandlimited).

While a variety of design parameters can be considered for the embedded communication component in (3), the THoRaCs procedure in [7] focused on three: namely 1) the symbol constellation, 2) the number of OFDM subcarriers N relative to waveform BT, and 3) the placement of these subcarriers within the radar spectrum. Regarding symbol constellations, 4-QAM, 16-QAM, and 64-QAM were examined as they are commonly used in OFDM applications. The number of embedded OFDM subcarriers is arbitrary, though it was shown in [7] that distortion of the modulated symbols increasingly occurs as N becomes a significant fraction of BT.

Finally, three different placement strategies for the OFDM subcarriers within the radar band were considered, with all limiting the N subcarriers to reside within the 3-dB bandwidth B. The "Contiguous Fixed" strategy places the subcarriers in N contiguous frequencies that remain fixed across all M pulses in the CPI. The "Contiguous Hopped" strategy likewise places the subcarriers in N contiguous frequencies for each pulse, though the location of the group is allowed to randomly hop on a pulse-to-pulse basis within the CPI. Finally, the "Non-contiguous Hopped" strategy allows the subcarriers to separately hop to any location (excluding overlap) within B for each pulse in the CPI. Synchronization of the hopping locations between the transmitter and receiver is obviously required for the second and third placement strategies.

Figure 1 illustrates an example of a 4-QAM symbol constellation in which OFDM subcarriers are demodulated from a set of $M = 10^3$ THoRaCs waveforms where $N = 50$ (25% of $BT = 200$) subcarriers per pulse are embedded via the "Contiguous Fixed" arrangement. While the demodulated symbols are grouped closely around their respective true constellation points, there is a small degree of spreading that arises from the design process (this result is simulated and does not contain noise). Specifically, the root-mean-square (RMS) error vector magnitude (EVM) [18], expressed as a percentage of the average symbol energy of the constellation, is 0.45% in this case.

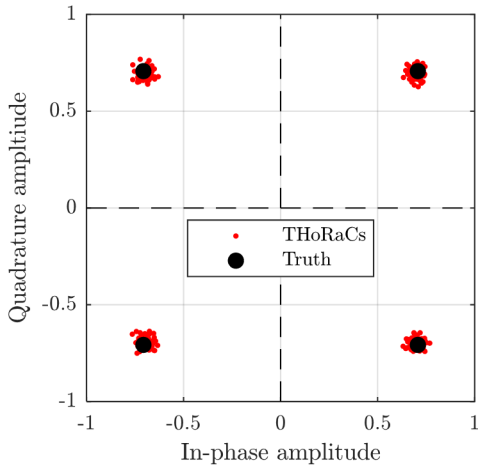

Fig. 1. Noise-free simulation of optimized 4-QAM symbol mapping of THoRaCs for $N = 50$ subcarriers (25% of BT)

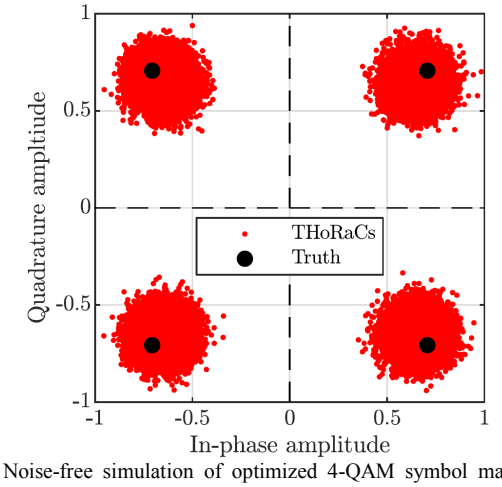

Fig. 2. Noise-free simulation of optimized 4-QAM symbol mapping of THoRaCs for $N = 150$ subcarriers (75% of BT)

To demonstrate the impact of OFDM distortion that can arise by enforcing (2), Figure 2 shows the same arrangement as Fig. 1 albeit with $N = 150$ subcarriers (75% of BT) in each THoRaCs pulse. Due to the final stage (6) of the design process the waveforms are still random FM and thus the expected radar performance is unchanged. However, as evidenced by Fig. 2, attempting to impose the fixed OFDM

structure (for the given set of arbitrary symbols) onto the waveform design results in degradation of symbol accuracy. The EVM in this case has increased to 10.9%, a factor of 24 increase over that of Fig. 1. Conceptually, the excess signal $e(t)$ simply does not possess enough degrees of freedom by itself to provide an FM signal structure for $s(t)$, and so $r(t)$ is altered as well.

As with standard communications, the presence of noise, fading, and multipath over a free-space link further hinder the receiver's ability to correctly determine the embedded symbols, thus necessitating channel equalization and possibly some manner of error correction. Given that these factors are unavoidable, the selection of N (as a percentage of BT) becomes an important decision in the practical implementation of this radar/communication emission scheme.

III. Experimental Results

A set of $M = 10^3$ pulsed waveforms having a time-bandwidth product of $BT = 200$ ($B = 66.7$ MHz and $T = 3$ μs) were designed according to (3)-(6). The collective CPI therefore has an effective BT of 2×10^5 that provides ~53 dB of coherent integration gain in the radar receiver.

Each test waveform was digitally upsampled to 10 GS/s in Matlab™ and up-converted to a center frequency of 3.55 GHz for physical generation on a Tektronix AWG70002A arbitrary waveform generator (AWG) at a pulse repetition frequency (PRF) of 25 kHz. The received signal (for either radar or communications) is I/Q sampled by a Rohde & Schwarz FSW Real-time Spectrum Analyzer (RSA) at a rate of 200 MS/s.

A. Experimental Radar Assessment

Open-air testing to assess the radar operation was performed from the roof of Nichols Hall on the University of Kansas campus. An MTI mode was evaluated using separate transmit and receive antennas pointed at the intersection of 23rd and Iowa streets, which contains ample motor vehicle traffic in a sufficiently radial orientation.

The reflections produced by each of the $M = 10^3$ transmitted waveforms are pulse compressed using a loopback-measured version of the waveform to account for any hardware distortion effects. Doppler processing using a Taylor window was subsequently performed along with a simple zero-Doppler projection clutter canceller (since the platform is stationary).

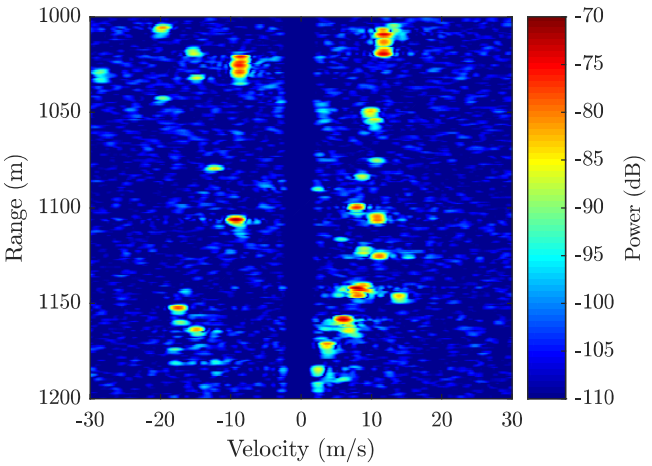

Fig. 3. Range-Doppler plot of experimentally illuminated moving targets by 1000 unique THoRaCs waveforms with $BT = 200$

Figure 3 shows the resulting range-Doppler plot for the particular case of optimized waveforms having $N = 50$ (25% of BT) subcarriers per pulse, independently modulated with equally probable random symbols from a 4-QAM constellation, and arranged according to the "Contiguous Fixed" strategy in the center of the band. It is observed that several moving vehicles are clearly visible and the background sidelobes are quite low due to their incoherent integration over the 1000 unique pulsed waveforms in the CPI. It has also been observed (not shown here) that designing waveforms according to each of the other parameter combinations considered in [7] yields results that are qualitatively indistinguishable from that in Fig. 3.

B. Loopback Experimental Communication Assessment

To establish an experimental performance baseline for the communication aspect of THoRaCs we first consider a simple loopback capture of each waveform in which the transmitter (AWG) is connected directly to the receiver (RSA). The AWG and RSA were referenced from the same clock to avoid synchronization effects and the hardwired channel does not exhibit multipath, thus also avoiding the need for equalization (these effects are addressed for the open-air measurements).

Figures 4-6 illustrate the 4-QAM, 16-QAM, and 64-QAM demodulated symbol constellations when embedded within 1000 unique THoRaCs waveforms having $N = 50$ (25% of BT) subcarriers per pulse arranged according to the "Contiguous Fixed" strategy in the center of the band (same as the radar assessment). Thus these cases correspond to respective data rates of 2.5 Mbps, 5.0 Mbps, and 7.5 Mbps. The EVM in these cases are 4.0%, 3.0% and 3.2%, respectively.

These cases illustrate excellent agreement with the true symbol values, which is expected since only 25% of BT is being devoted to embedding information and thus there is sufficient design freedom to effectively avoid the error-causing distortion that was observed in Fig. 2. The constellation density also does not appear to be introducing any appreciable distortion when the waveforms are physically implemented because all three loopback captures were demodulated with no symbol errors. Had errors been observed, they could only have been attributable to waveform distortion since the loopback arrangement is essentially noise-free.

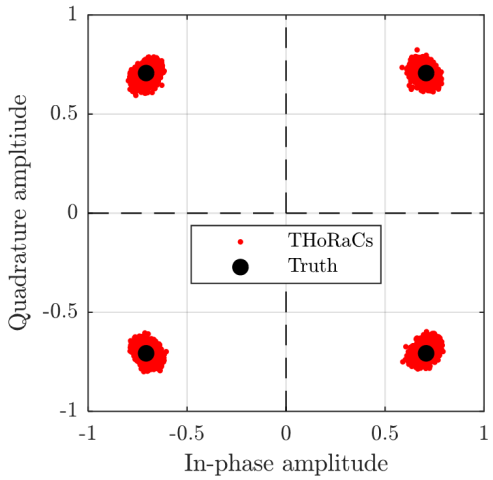

Fig. 4. Demodulated 4-QAM constellation after loopback capture

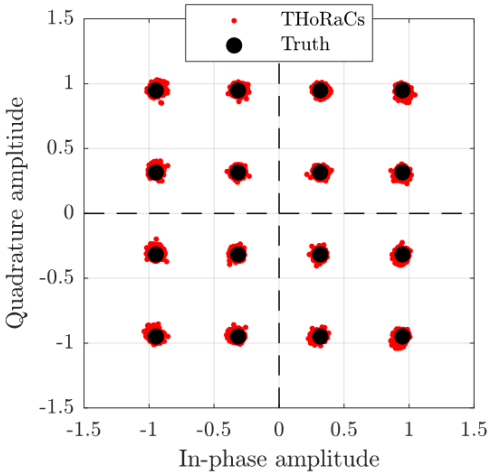

Fig. 5. Demodulated 16-QAM constellation after loopback capture

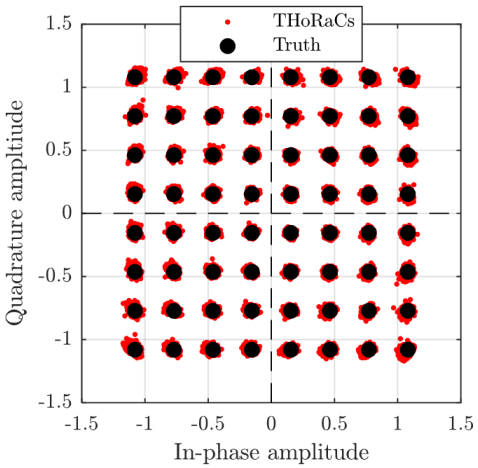

Fig. 6. Demodulated 64-QAM constellation after loopback capture

C. Open-Air Synchronization and Equalization

For THoRaCs waveforms to operate in an open-air environment as their dual-function nature intends, it is necessary for the communication receiver to perform synchronization and channel estimation/equalization based on known pilot symbols prior to determination of the information-bearing symbols. Since the embedded communication signal in (3) does not include the usual OFDM cyclic prefix, which is expected to otherwise introduce ambiguities in the form of increased radar range sidelobes, standard OFDM frequency domain equalization would most likely realize some degradation due to mismatch effects. Instead, channel equalization was performed by estimating the inverse of the channel response with a Wiener Filter (WF) and then forming an inverse filter using a zero-forcing (ZF) equalizer.

Denote the signal captured at the communication receiver as

$$y(t) = s(t) * g(t) + v(t) \tag{7}$$

in which $g(t)$ is the impulse response of the one-way communication channel and $v(t)$ is additive white Gaussian noise (AWGN). In discretized form the WF estimate of the channel is therefore [19]

$$\hat{\mathbf{g}} = \mathbf{R}^{-1}\mathbf{p}\,, \tag{8}$$

for $\mathbf{R}$ the autocorrelation matrix of $s(t)$ and $\mathbf{p}$ the cross-correlation between $s(t)$ and $y(t)$. Clearly the determination of these terms requires that the given waveform be known at the communication receiver (i.e. a "pilot waveform").

Using the WF channel estimate from (8) the well-known ZF equalizer can then be realized via [20]

$$\mathbf{c} = (\mathbf{A}^H\mathbf{A} + \sigma\mathbf{I})^{-1}\mathbf{A}^H\mathbf{e} \tag{9}$$

where $\mathbf{I}$ is an identity matrix, σ is a small loading factor, $\mathbf{e}$ is an elementary vector with a '1' in the middle element and zeros elsewhere, and the matrix

$$\mathbf{A} = \begin{bmatrix} \hat{\mathbf{g}} & 0 & \cdots & 0 \\ 0 & \hat{\mathbf{g}} & \ddots & \vdots \\ \vdots & \ddots & \ddots & 0 \\ 0 & \cdots & 0 & \hat{\mathbf{g}} \end{bmatrix}. \tag{10}$$

The ZF equalizer in (9) can then be applied to the discretized version of (7) to compensate for channel distortion.

D. Open-Air Experimental Communication Assessment

The same three sets of 1000 THoRaCs waveforms evaluated in loopback were transmitted in open-air on the back lawn of Nichols Hall on the University of Kansas campus. The placement of the transmit and receive antennas is shown in Fig. 7. The antennas are separated by approximately 50 meters and possess a line-of-sight (LOS) path. As with the loopback measurements, the AWG feeds the transmit antenna and the RSA is used to obtain the signal captured by the receive antenna. Unlike the loopback measurements, no common clock reference exists and there is some multipath due to ground bounce and nearby buildings/trees.

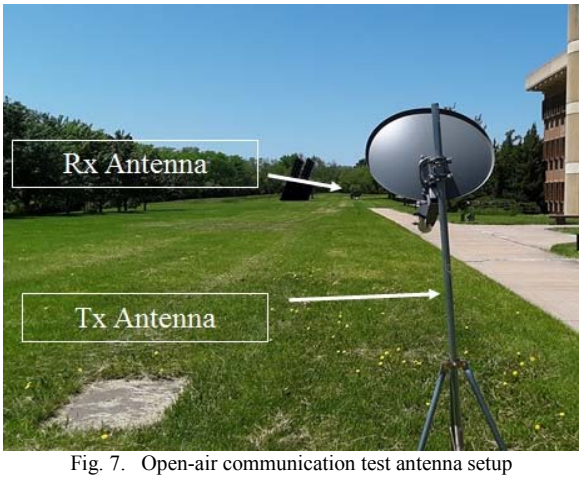

Fig. 7. Open-air communication test antenna setup

For each set of a 1000 waveforms, every 50th pulse serves as a pilot waveform to perform channel estimation/equalization via (8)-(10) after RSA capture, and is then applied to the subsequent 49 received pulses. It is also necessary to estimate the frequency offset that naturally arises because the transmitter and receiver have separate clocks and thus cannot be perfectly synchronized. Because this offset tends to be relatively small, the pulsed configuration permits a pulse-to-pulse phase change to be estimated between consecutive pulses. For this experimental assessment the 1st and 2nd pulses out of each set of 1000

were employed as pilots to determine this phase offset (with some error of course) that was subsequently used to compensate all other pulses for frequency offset in a progressive manner. When channel re-estimation occurs at each 50th pulse the progressive frequency offset compensation is likewise restarted to address the inevitable error-induced phase drift.

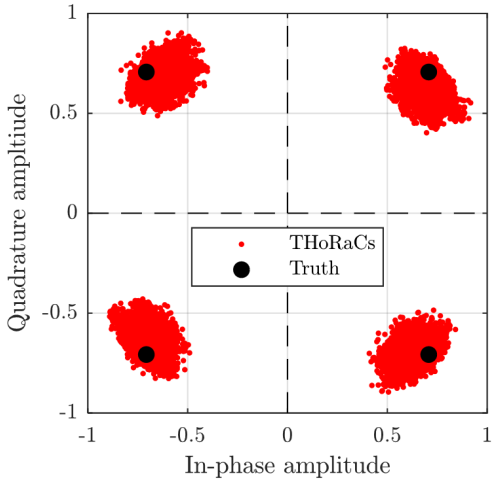

Fig. 8. Demodulated 4-QAM constellation for free-space scenario

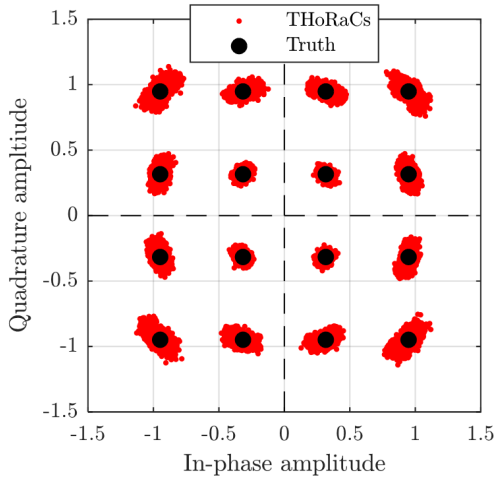

Fig. 9. Demodulated 16-QAM constellation for free-space scenario

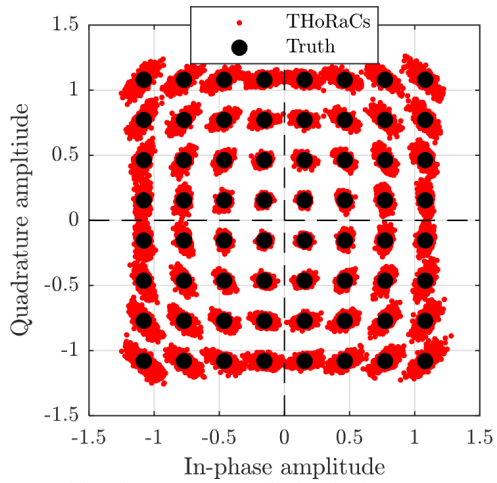

Fig. 10. Demodulated 64-QAM constellation for free-space scenario

Figures 8-10 show the 4-QAM, 16-QAM, and 64-QAM demodulated symbol constellations, respectively, after open-air capture and subsequent synchronization/equalization. The EVM in these cases are 10.2%, 5.6% and 5.2%, respectively, representing increases by 2.6×, 1.9×, and 1.6× over their loopback capture counterparts in Figs. 4-6. Compared to the loopback captures in Figs. 4-6 an expected increased spreading about the true symbol values is observed. Moreover, the prominent phase-orientated nature of this spreading can likely be attributed to the rather crude approach taken for frequency offset estimation and subsequent synchronization.

There was insufficient data to measure a non-zero SER for the 4-QAM and 16-QAM case in this open-air test, though the 64-QAM case did realize an SER of 1.8×10^{-3} (excluding the 20 pilot waveforms). Compared to the corresponding simulated analysis in Fig. 9 of [7], these results (albeit crude) agree with the high SNR regime (for communications) of 20 dB or so.

IV. Conclusions

Experimental communication results along with measured radar performance clearly demonstrate that THoRaCs represents a viable approach to embedding an information-bearing payload into radar waveforms while preserving the efficacy of the radar mission. This evaluation involved standard channel estimation/equalization, a rather unsophisticated approach to frequency offset estimation for synchronization, and no form of error correction coding. It therefore stands to reason that more sophisticated techniques could be incorporated into the communication component, including the possibility of various forms of MIMO (noting the benefits to radar and communication can be quite different in this regard [21]).

Finally, further experimental assessment is needed to understand the impact that nonlinear distortion by a truly high-power transmitter could cause [4]. While FM waveforms theoretically only reside at a single instantaneous frequency, memory effects in the transmitter still produces some degree of intermodulation. The inherent nonrepeating nature of these waveforms make them rather robust to these degradations from a radar perspective as long as adequate loopback capture of the amplified waveform is available with sufficient fidelity. It remains to be seen, however, how the communication component will fare.

References

[1] A. Hassanien, M.G. Amin, Y.D. Zhang, F. Ahmad, "Signaling strategies for dual-function radar communications: an overview," *IEEE AESS Systems Magazine*, vol. 31, no. 10, pp. 36-45, Oct. 2016.

[2] S.D. Blunt, E.L. Mokole, "An overview of radar waveform diversity," *IEEE AESS Systems Magazine*, vol. 31, no. 11, pp. 2-42, Nov. 2016.

[3] S.D. Blunt, E.S. Perrins, *Radar & Communication Spectrum Sharing*, SciTech Publishing, 2018.

[4] H. Griffiths, L. Cohen, S. Watts, E. Mokole, C. Baker, M. Wicks, S. Blunt, "Radar spectrum engineering and management: technical and regulatory Issues," *Proc. IEEE*, vol. 103, no. 1, pp. 85-102, Jan. 2015.

[5] J. Jakabosky, B. Ravenscroft, S.D. Blunt, A. Martone, "Gapped spectrum shaping for tandem-hopped radar/communications & cognitive sensing," *IEEE Radar Conf.*, Philadelphia, PA, May 2016.

[6] B. Ravenscroft, P.M. McCormick, S.D. Blunt, J. Jakabosky, J.G. Metcalf, "Tandem-hopped OFDM communications in spectral gaps of FM noise radar," *IEEE Radar Conf.*, Seattle, WA, May 2017.

[7] B. Ravenscroft, P. M. McCormick, S. D. Blunt, E. Perrins, J.G. Metcalf, "A power-efficient formulation of tandem-hopped radar & communications," *IEEE Radar Conf.*, Oklahoma City, OK, Apr. 2018.

[8] J. Jakabosky, S.D. Blunt, B. Himed, "Spectral-shape optimized FM noise radar for pulse agility," *IEEE Radar Conf.*, Philadelphia, PA, May 2016.

[9] C. Sahin, J. Jakabosky, P. McCormick, J. Metcalf, S.D. Blunt, "A novel approach to embed communication symbols into physical radar waveforms," *IEEE Radar Conf.*, Seattle, WA, May 2017.

[10] J. Owen, S.D. Blunt, K. Gallagher, P. McCormick, C. Allen, K. Sherbondy, "Nonlinear radar via intermodulation of FM noise waveform pairs," *IEEE Radar Conf.*, Oklahoma City, OK, Apr. 2018.

[11] C.A. Mohr, P.M. McCormick, S.D. Blunt, "Optimized complementary waveform subsets within an FM noise radar CPI," *IEEE Radar Conf.*, Oklahoma City, OK, Apr. 2018.

[12] B. Ravenscroft, J.W. Owen, J. Jakabosky, S.D. Blunt, A.F. Martone, K.D. Sherbondy, "Experiemental demonstration and analysis of cognitive spectrum sensing and notching for radar," *IET Radar, Sonar & Navigation*, vol. 12, no. 12, pp. 1466-1475, Dec. 2018.

[13] C.A. Mohr, S.D. Blunt, "FM noise waveforms optimized according to a temporal template error (TTE) metric," *IEEE Radar Conf.*, Boston, MA, Apr. 2019.

[14] C.A. Mohr, S.D. Blunt, "Design and generation of stochastically defined, pulsed FM noise waveforms," *Intl. Radar Conf.*, Toulon, France, Sept. 2019.

[15] S.C. Thompson, A.U. Ahmed, J.G. Proakis, J.R. Zeidler, M.J. Geile, "Constant envelope OFDM," *IEEE Trans. Communications*, vol. 56, no. 8, pp. 1300-1312, Aug. 2008.

[16] S.C. Thompson, J.P. Stralka, "Constant envelope OFDM for power-efficient radar and data communications," *Intl. Waveform Diversity & Design Conf.*, Kissimmee, FL, Feb. 2009.

[17] M.P. Wylie-Green, E. Perrins, T. Svensson, "Introduction to CPM-SC-FDMA: a novel multiple-access power-efficient transmission scheme," *IEEE Trans. Communications*, vol. 59, no. 7, pp. 1904-1915, July 2011.

[18] S.R. Bullock, *Transceiver and System Design for Digital Communications*, SciTech Publishing, 2009, pp. 58.

[19] S. Haykin, *Adaptive Filter Theory*, Pearson Education, 2014, Chap. 2.

[20] U. Madhow, ed., *Fundamentals of Digital Communication*, Cambridge University Press, 2008, Chap. 5.

[21] F. Daum, J. Huang, "MIMO radar: snake oil or good idea?," *IEEE Aerospace & Electronic Systems Mag.*, vol. 24, no. 5, pp. 8-12, May 2009.